Intra-Arterial Transplantation of Stem Cells in Large Animals – A Minimally-Invasive Strategy for the Treatment of Disseminated Neurodegeneration

Izabela Malysz-Cymborska (i.m.cymborska@gmail.com)
Department of Neurosurgery, School of Medicine, Collegium Medicum, University of Warmia and Mazury, Olsztyn

Dominika Golubczyk
Department of Neurosurgery, School of Medicine, Collegium Medicum, University of Warmia and Mazury, Olsztyn

Lukasz Kalkowski
Department of Neurosurgery, School of Medicine, Collegium Medicum, University of Warmia and Mazury, Olsztyn

Joanna Kwiatkowska
Department of Neurosurgery, School of Medicine, Collegium Medicum, University of Warmia and Mazury, Olsztyn

Michal Zawadzki
Central Clinical Hospital of Ministry of the Interior and Administration in Warsaw

Joanna Glodek
Department of Surgery and Radiology, Faculty of Veterinary Medicine, University of Warmia and Mazury, Olsztyn

Piotr Holak
Department of Surgery and Radiology, Faculty of Veterinary Medicine, University of Warmia and Mazury, Olsztyn

Joanna Sanford
Sanford Biotech, Warsaw

Kamila Milewska
Department of Neurosurgery, School of Medicine, Collegium Medicum, University of Warmia and Mazury, Olsztyn

Zbigniew Adamiak
Department of Surgery and Radiology, Faculty of Veterinary Medicine, University of Warmia and Mazury, Olsztyn

Piotr Walczak
Center for Advanced Imaging Research and Department of Diagnostic Radiology and Nuclear Medicine, University of Maryland School of Medicine, Baltimore, MD

Miroslaw Janowski
Center for Advanced Imaging Research and Department of Diagnostic Radiology and Nuclear Medicine, University of Maryland School of Medicine, Baltimore, MD

Research Article

Keywords: intra-arterial, therapeutic, neurological, MSCs

Posted Date: December 4th, 2020

DOI: https://doi.org/10.21203/rs.3.rs-114224/v1

Version of Record: A version of this preprint was published at Scientific Reports on March 22nd, 2021. See the published version at https://doi.org/10.1038/s41598-021-85820-3.

Abstract

Stem cell transplantation proved promising in animal models of neurological diseases; however, in conditions with disseminated pathology such as ALS, delivery of cells and their broad distribution is challenging. To address this problem, we explored intra-arterial (IA) delivery route of stem cells. The goal of this study was to investigate the feasibility and safety of MRI-guided transplantation of glial restricted precursors (GRPs) and mesenchymal stem cells (MSCs) in dogs suffering from ALS-like disease, degenerative myelopathy (DM). Three naïve pigs were used for MSC transplantation as a pre-treatment control before transplantation in dogs. Cells were labeled with iron oxide nanoparticles. For IA transplantation a 1.2-French microcatheter was advanced into the middle cerebral artery under roadmap guidance. Then, the cells were transplanted under real-time MRI with the acquisition of dynamic T2*-weighted images. Interventional and follow-up MRI proved the procedure was feasible and safe. The transplantation of canine GRPs resulted in rather poor retention in the brain, whereas canine MSCs demonstrated excellent settlement. Notably, histopathology showed the successful and predictable placement of transplanted porcine MSCs. Analysis of gene expression after transplantation revealed a reduction of inflammatory factors, which may indicate a promising therapeutic strategy in the treatment of neurodegenerative diseases.

Introduction

The central nervous system (CNS) is by far the most challenging therapeutic target, and its endogenous regenerative capacity is minimal. Usually the prognoses of patients suffering from neurological disorders are dire, elevating pressure to develop new therapeutic strategies. One of the most controversial approaches of the last several decades has been the use of stem cells[1,2]. The potential of stem cells has enthralled the world, but more than thirty years after the first clinical trials, outcomes are rather disappointing. This is despite impressive progress with the identification of compelling therapeutic targets such as replacement of glia[3] or isolation of highly potent stem cell sources such as primary neural stem cells[4]. There is a growing consensus that the reason behind the suboptimal therapeutic effect of otherwise highly potent stem cells is their inadequate delivery. There are several gateways to the brain, but the most common route of stem cell administration is intravenous (IV) infusion [5,6]. While easy to perform, non-invasive and safe, the IV route has proven to result in very low efficacy of cell accumulation in the brain[7]. To address these shortcomings, the intra-arterial (IA) route has been utilized as much more effective, taking advantage of the first pass trapping effect resulting in excellent cell accumulation in the brain[8]. Over the last decade significant advances have been made using targeted IA delivery, including robust technology for image-guidance to improve reproducibility, precision and safety of targeted IA administration [9]. Real-time image-guided MRI targeting of therapeutic agents enables delivering therapy to a selected region of the brain with high accuracy and reproducibility. Unique to IA administration, therapeutics can be distributed at high concentrations, broadly and uniformly throughout the targeted brain territory, and with minimal systemic exposure [10]. Image-guided targeting of cells globally to the entire central nervous system creates the opportunity to make significant advancements in

developing a breakthrough treatment for diseases with disseminated pathology such as amyotrophic lateral sclerosis (ALS). The most common approach to pre-clinical modeling of ALS is genetic rodent models [11,12]. While they represent a valuable and cost-effective strategy for the initial screening of therapeutic compounds, a direct translation of outcomes from small animals to humans led to many failed clinical studies. In response to this problem, we decided to use a unique human ALS model – dogs with naturally occurring degenerative myelopathy (DM)[3,4]. The size of the brain, the environment shared with humans, and the natural occurrence of the disease are more representative of human conditions and, as such, provide an excellent model that bridges rodent and clinical studies.

Moreover, the size and the cerebral vasculature of the dog brain enables navigation of IA catheters towards distal cerebral vessels and targeted delivery of stem cells under the guidance of clinical imaging equipment, further improving clinical relevance. Considering the advantages mentioned above of the image-guided IA route, we utilized this strategy to deliver stem cells directly to the brain in dogs suffering from DM. The primary goal of this study was to show the feasibility and safety of image-guided IA delivery route to the brain. As therapeutic agents, we used two major classes of stem cells: glial restricted precursors (GRPs) with therapeutic effect demonstrated in rodent models of ALS [12,13], and mesenchymal stem cells (MSCs) with demonstrated broad trophic and immunomodulatory effects[14].

Results

Intra-arterial MRI-guided transplantation of canine GRPs (cGRPs) in DM dogs

Dogs with their internal carotid artery cannulated under X-ray angiography were placed in 3T MRI for MRI-guided injection. Prior to cell transplantation, trans-catheter perfusion territory was visualized using the IA injection of Feraheme contrast (AMAG pharmaceuticals, Waltham, USA) and the infusion rate was adjusted to achieve adequate coverage throughout the ipsilateral hemisphere. cGRPs were injected IA while acquiring dynamic GE-EPI scans using the infusion speed that was predetermined by contrast agent pre-injection. During cGRP infusion, signal intensity change was observed in the ipsilateral cortex, indicating labeled cells entered cortical circulation (**Fig. 1 A**). Quantitative analysis of the dynamic scans revealed that the maximum signal was found at the end of infusion (35s). Immediately upon infusion completion, it rapidly cleared, suggesting that cells were not captured by cerebral endothelium and perfused out (**Fig. 1 A, D**). Brain territory with a hypointense signal indicating localization of cGRP cells during vs. after transplantation was 7.017 ±0.39 cm^2 and 2.271 ± 2.041 cm^2, respectively, which confirms that the brain area covered with cells had been reduced by 74.11% (**Fig. 1 A**; $P < 0.001$).

Intra-arterial MRI-guided transplantation of porcine MSCs (pMSCs) in pigs

IA transplantation of small cGRPs in dogs showed weak cell homing in the brain; thus, we decided to use MSCs, which are more significant and known for better homing. MSCs have been associated with microembolic complications; hence before their use in companion DM dogs, the safety of the selected dose was tested in pigs. IA catheter was placed under X-ray angiography in the pharyngeal ascendant

artery just proximal to rete (**Fig. 2 A**). Dynamic MRI during cell infusion revealed extensive signal intensity change throughout the ipsilateral hemisphere, delineating flow and distribution of SPION-labeled MSCs (**Fig. 1 B**). The hypointense signal of pMSCs at the end of the injection, expressed in a relative number of pixels, decreased only by 31.25±2.10 % compared to the initial value (**Fig. 1 B**). This indicates excellent endothelial capture and settlement of MSCs in the brain following IA pMSC transplantation.

Real-time MRI monitored cMSCs intra-arterial transplantation in DM dogs

Based on data obtained during MSC transplantation in pigs, we proceeded to transplant canine MSCs in DM dogs. The cMSCs labeled with SPION were injected when the dog was inside the MRI scanner with dynamic imaging showing cogent accumulation of cells throughout the ipsilateral hemisphere (**Fig. 1 C, 2 B**). There was a gradual accumulation of the hypointense pixels with the maximum signal detected towards the end of cMSCs' infusion. Cells covered 7.375 ± 0.3084 cm^2 of hemisphere during injection and 6.296 ± 0.4270 cm^2 at the end of the infusion, which means that clearance of cells after completed injection was only 15% (**Fig. 1 C, E**). This indicates that cMSCs were captured very well by cerebral endothelium.

Safety of intra-arterial cell transplantation

It has been shown that the IA injection of MSCs is associated with the risk of microembolism when an excessive number of cells are infused. To examine the safety of transplantation, we performed diffusion scans, particularly focusing on regions with high cell uptake and did not observe any focal or diffuse abnormalities on SWI and ADC maps neither in pigs grafted with pMSCs or dogs following cMSC injections (**Fig. 2 C**, **D** and **E**, **F** respectively). Quantitative assessment of signal intensity histograms of selected ROIs for both ipsilateral and contralateral hemispheres showed the accumulation of hypointense pixels on SWI in the ipsilateral hemisphere (**Fig. 2 C'** and **D'**) compared to the contralateral hemisphere (**Fig. 2 C"** and **D"**). Histogram did not show any changes in diffusion on ADC maps after cell transplantation (**Fig.2 E'-F"**). To examine whether the transplantation procedure led to chronic focal effects such as brain atrophy, measurements of hemispheric and ventricular symmetry were performed before surgery and a few months after cell transplantation. No statistically significant difference in symmetry has been detected before vs. after therapy with GRPs (P=0.86, P=0.86 for left and right hemisphere respectively; P=0.48 and P=0.51 for left and right ventricle respectively; **Fig. 2 G**) or MSCs (P=0.76, P=0.84 for left and right hemisphere respectively; P=0.53, P**=**0.55 for left and right ventricle respectively; **Fig. 2 H**). Clinically, there was no evidence of focal damage, hemorrhage or stroke in T2w MRI neither in the dogs treated with GRPs (**Fig. 2 G**) nor in those treated with MSCs (**Fig. 2 H**).

Histological detection of transplanted pMSCs in swine

Histopathological analysis confirmed the distribution of pMSCs in regions shown during interventional MRI - guided pMSC transplantation procedure. Prussian blue staining facilitated detection of iron oxide nanoparticles present in pMSCs in the ipsilateral hemisphere (**Fig. 3 B, B'**) and lack of positive cells in the

contralateral hemisphere (**Fig. 3 A, A'**). This presence of cells only in the ipsilateral hemisphere further demonstrates that cells entering circulation do not re-enter the brain.

Impact of cMSCs transplantation on gene expression in DM dogs

With an effort to get an initial insight into potential therapeutic effects, we analyzed the expression of several transcripts in the brain that are of key importance in the context of neuronal and glial function and neurodegenerative processes. In dogs treated with MSCs, we observed decreased Iba-1 ($P < 0.5$) and GFAP ($P < 0.01$) mRNA expression in the ipsilateral compared to the contralateral (untreated) hemisphere. The MCT2 mRNA expression was increased in the hemisphere transplanted with cMSCs compared to the non-transplanted hemisphere (**Fig. 4**). We didn't observe any change of Olig1 or Olig2, MBP, ChaT, MCT4, and RbFox3 mRNA expression after cMSC transplantation.

Intra-arterial MRI-guided transplantation of canine GRPs (cGRPs) in DM dogs

Dogs with their internal carotid artery cannulated under X-ray angiography were placed in 3T MRI for MRI-guided injection. Prior to cell transplantation, trans-catheter perfusion territory was visualized using the IA injection of Feraheme contrast (AMAG pharmaceuticals, Waltham, USA) and the infusion rate was adjusted to achieve adequate coverage throughout the ipsilateral hemisphere. cGRPs were injected IA while acquiring dynamic GE-EPI scans using the infusion speed that was predetermined by contrast agent pre-injection. During cGRP infusion, signal intensity change was observed in the ipsilateral cortex, indicating labeled cells entered cortical circulation (**Fig. 1 A**). Quantitative analysis of the dynamic scans revealed that the maximum signal was found at the end of infusion (35s). Immediately upon infusion completion, it rapidly cleared, suggesting that cells were not captured by cerebral endothelium and perfused out (**Fig. 1 A, D**). Brain territory with a hypointense signal indicating localization of cGRP cells during vs. after transplantation was 7.017 ±0.39 cm^2 and 2.271 ± 2.041 cm^2, respectively, which confirms that the brain area covered with cells had been reduced by 74.11% (**Fig. 1 A**; $P < 0.001$).

Intra-arterial MRI-guided transplantation of porcine MSCs (pMSCs) in pigs

IA transplantation of small cGRPs in dogs showed weak cell homing in the brain; thus, we decided to use MSCs, which are more significant and known for better homing. MSCs have been associated with microembolic complications; hence before their use in companion DM dogs, the safety of the selected dose was tested in pigs. IA catheter was placed under X-ray angiography in the pharyngeal ascendant artery just proximal to rete (**Fig. 2 A**). Dynamic MRI during cell infusion revealed extensive signal intensity change throughout the ipsilateral hemisphere, delineating flow and distribution of SPION-labeled MSCs (**Fig. 1 B**). The hypointense signal of pMSCs at the end of the injection, expressed in a relative number of pixels, decreased only by 31.25±2.10 % compared to the initial value (**Fig. 1 B**). This indicates excellent endothelial capture and settlement of MSCs in the brain following IA pMSC transplantation.

Real-time MRI monitored cMSCs intra-arterial transplantation in DM dogs

Based on data obtained during MSC transplantation in pigs, we proceeded to transplant canine MSCs in DM dogs. The cMSCs labeled with SPION were injected when the dog was inside the MRI scanner with dynamic imaging showing cogent accumulation of cells throughout the ipsilateral hemisphere (**Fig. 1 C, 2 B**). There was a gradual accumulation of the hypointense pixels with the maximum signal detected towards the end of cMSCs' infusion. Cells covered 7.375 ± 0.3084 cm^2 of hemisphere during injection and 6.296 ± 0.4270 cm^2 at the end of the infusion, which means that clearance of cells after completed injection was only 15% (**Fig. 1 C, E**). This indicates that cMSCs were captured very well by cerebral endothelium.

Safety of intra-arterial cell transplantation

It has been shown that the IA injection of MSCs is associated with the risk of microembolism when an excessive number of cells are infused. To examine the safety of transplantation, we performed diffusion scans, particularly focusing on regions with high cell uptake and did not observe any focal or diffuse abnormalities on SWI and ADC maps neither in pigs grafted with pMSCs or dogs following cMSC injections (**Fig. 2 C**, **D** and **E**, **F** respectively). Quantitative assessment of signal intensity histograms of selected ROIs for both ipsilateral and contralateral hemispheres showed the accumulation of hypointense pixels on SWI in the ipsilateral hemisphere (**Fig. 2 C'** and **D'**) compared to the contralateral hemisphere (**Fig. 2 C"** and **D"**). Histogram did not show any changes in diffusion on ADC maps after cell transplantation (**Fig.2 E'-F"**). To examine whether the transplantation procedure led to chronic focal effects such as brain atrophy, measurements of hemispheric and ventricular symmetry were performed before surgery and a few months after cell transplantation. No statistically significant difference in symmetry has been detected before vs. after therapy with GRPs (P=0.86, P=0.86 for left and right hemisphere respectively; P=0.48 and P=0.51 for left and right ventricle respectively; **Fig. 2 G**) or MSCs (P=0.76, P=0.84 for left and right hemisphere respectively; P=0.53, P**=**0.55 for left and right ventricle respectively; **Fig. 2 H**). Clinically, there was no evidence of focal damage, hemorrhage or stroke in T2w MRI neither in the dogs treated with GRPs (**Fig. 2 G**) nor in those treated with MSCs (**Fig. 2 H**).

Histological detection of transplanted pMSCs in swine

Histopathological analysis confirmed the distribution of pMSCs in regions shown during interventional MRI - guided pMSC transplantation procedure. Prussian blue staining facilitated detection of iron oxide nanoparticles present in pMSCs in the ipsilateral hemisphere (**Fig. 3 B, B'**) and lack of positive cells in the contralateral hemisphere (**Fig. 3 A, A'**). This presence of cells only in the ipsilateral hemisphere further demonstrates that cells entering circulation do not re-enter the brain.

Impact of cMSCs transplantation on gene expression in DM dogs

With an effort to get an initial insight into potential therapeutic effects, we analyzed the expression of several transcripts in the brain that are of key importance in the context of neuronal and glial function and neurodegenerative processes. In dogs treated with MSCs, we observed decreased Iba-1 ($P < 0.5$) and GFAP ($P < 0.01$) mRNA expression in the ipsilateral compared to the contralateral (untreated) hemisphere.

The MCT2 mRNA expression was increased in the hemisphere transplanted with cMSCs compared to the non-transplanted hemisphere (**Fig. 4**). We didn't observe any change of Olig1 or Olig2, MBP, ChaT, MCT4, and RbFox3 mRNA expression after cMSC transplantation.

Discussion

Over the past decade, there has been tremendous progress in the area of IA therapies, mainly fueled by advances in the treatment of ischemic stroke, but also in the delivery of therapeutics and stem cells to various organs[15,16]. The IA route was shown to be safe and cell targeting efficiency was superior compared to the IV route in animal models [17]. Cannulation of MCA via ICA in dogs was successful using 1.2 F microcatheter in contrast to Camstra et al. [18] who reported frequent vasospasms while transitioning through tortuosities of ICA. We have demonstrated an excellent safety profile for the GRP delivery procedure in all transplanted animals. Thanks to dynamic, real-time MRI monitoring during cell infusion, it was possible to visualize the process of cell entrapment in the brain. This enables early intervention should any excessive accumulation and blockage of cerebral flow occur. The MRI scans did not show any abnormalities indicating microhemorrhages or stroke right after the transplantation or even after several months of follow up. However, the accumulation of GRP cells in the brain was very low. Most of the cells perfused away from the brain just after the infusion was completed. These results were in agreement with Lundberg et al[19], who showed poor human neural progenitors (hNPCs) and rat NPC recruitment in rat brains after IA transplantation in contrast to human MSCs. To address this problem, cells need to be either sorted for those with high expression of adhesion molecules[20] or engineered to artificially induce expression of adhesion receptors[21,22].

As the second class of widely used therapeutic cells, we used MSCs, which are larger in size and well known for their broad-based therapeutic mechanisms and high expression of adhesion molecules [23]. We previously utilized labeling and tracking of MSCs after transplantation in large animals[10], and here we used this approach to examine the safety of the method and efficacy of pMSCs' brain colonization in naive pigs.

To date, several studies of MSCs transplantated IA revealed adverse effects including reduced cerebral blood flow (CBF), increased mortality, and neurological impairment[24]. Given the fact that MSCs are significant, a key role in maintaining CBF and avoiding stroke is optimizing the velocity of administration and cell dose. Rat studies showed that the treatment of MSCs administered IA had a direct effect on reducing CBF[25]. Moreover, even low infusion velocity of MSCs was associated with many complications like necrotic cell-loss and blood brain barrier leakage[26]. Similarly, the dose of MSCs as well as pericyte-progenitor cells infused IA had a critical role in microembolic complications in dogs[27,28]. Considering the potential difficulties regarding CBF after the IA administration of cells demonstrated in small and large animal models, we decided to evaluate the safety of the method first on pigs.

We did not observe any adverse effects following transplantation, and brain accumulation of pMSCs was excellent. This outcome, based on dynamic MR imaging, was further confirmed by histology, where we found an abundance of pMSCs in the areas which correlated with MRI scans obtained on the day of administration. Subsequent experiments with transplantation of cMSCs in dogs with DM also showed excellent safety despite robust cell retention following transplantation. Much higher retention compared to GRPs is likely due to the larger size of MSCs or by the higher expression of adhesion molecules [22,29]. In comparison, the primary focus of this work demonstrating the feasibility and safety of the IA delivery focal localization of injected cells in the ipsilateral hemisphere offered a unique opportunity to gain insight into potential therapeutic effects. With cGRPs not accumulating in the brain in sufficient numbers, we focused this analysis on cMSCs. Based on tissues of dogs that succumb to DM, we observed a reduction in transcripts for IBA and GFAP, indicating the anti-inflammatory effect of cMSCs[30]. Because degenerative myelopathy, like ALS in humans, is correlated with inflammation, mainly present in the CNS [31], MSC transplantation via the IA route can be an excellent anti-inflammatory therapy in such diseases, as confirmed in our current research.

To summarize, our study demonstrated that IA injection of stem cells is safe and, in the case of MSCs, results in excellent cell accumulation in the brain making it an attractive route for delivery in neurodegenerative diseases like ALS. It represents an essential next step towards clinical use in ALS patients. However, for cells not equipped with an appropriate set of adhesion molecules, taking full advantage of this route will require cell engineering.

Material And Methods

Isolation of pMSCs

The pMSCs were isolated as described previously [4]. Bone marrow (BM) was aspirated from juvenile pig iliac crest using a syringe containing 10ml PBS with 200µl heparin (Polfa, Warsaw, Poland). The BM was diluted with PBS (Gibco, Gaithersburg, USA)) in a ratio of 1:2. Next, the mixture was layered on a Ficoll-Paque Plus (Sigma Aldrich, LGC Standards, UK) and centrifuged at 1300rpm at room temperature (RT) for 25 min. A ring of mononuclear cells was collected into a new tube with 20ml of PBS and centrifuged at 1500 rpm for 10 min in RT. Next, the pellet of cells was washed twice with PBS. Cells were suspended in the BMMSC medium (Gibco) and plated on 25ml flasks at 37°C in a humified incubator with 5% CO_2. Cultured cells were maintained for 15-20 days (2-3 passages), harvested with Accutase (Gibco), cryopreserved in a freezing medium (Sigma Aldrich), and stored in vapor-phase liquid nitrogen.

Isolation of cGRPs and cMSCs

cGRPs were isolated from canine fetuses between E32-37, as described previously[4]. For cMSC isolation, the lower abdomen adipose tissue was isolated during the sterilization of the bitch, with the agreement of the owner. The adipose tissue was washed with PBS (Gibco) 3 times and treated with Collagenase II (Gibco) for 3 hours at 37°C. Next, the collagenase was neutralized with serum from the donor and

centrifuged at 1550 rpm for 10 min in RT. The pellet was then passed through cell strainers, washed with PBS, and centrifuged at 1350 rpm for 10 min twice. Then, the cells were counted and cryopreserved in a freezing medium (Sigma Aldrich,), and stored in vapor-phase liquid nitrogen until used.

Animals

All animal experiments were approved by the University of Warmia and Mazury's ethics committee. The ARRIVE guidelines was followed for all animal studies. Experiments were performed according to the EU Directive 2010/63/EU as well as Poland Act 2015/01/15 "Act on the protection of animals used for scientific or educational purposes". Additionally, for transplantation procedures on dogs, written permission of dog owners was obtained.

Experimental Animals (Pigs)

Three juvenile, Large White domestic pigs (40kg, both sexes) were used. At least two weeks before transplantation, animals were acclimated to the new environment and human presence to minimize the stress associated with the experiment. Pigs had access to water and food *ad libitum*.

Experimental Animals (Dogs)

Eight dogs were recruited for the study based on neurological exam identifying symptoms of DM and genetic test confirming mutations in the SOD-1 gene, for immunosuppression dogs received cyclosporin (Equoral, Teva Pharmaceuticals, Poland), as described previously[4].

Cell preparation for the transplantation procedure

All types of cells (cGRP, cMSC, pMSC) were thawed three days before transplantation and plated on cell culture bottles in dedicated media. One day before transplantation, the medium was supplemented with 25 µg/ml SPION particles (Molday, BioPal, Worcester, MA, USA) for labeling and detection in MRI. The next day cells were washed with phosphate buffered saline (PBS), harvested, and centrifuged at 1100 rpm for 5 min. For transplantation, the cells pellet was suspended in PBS (4-5x10^6/ml).

MRI-guided intra-arterial transplantation of pMSCs

During the transplantation procedure, animals were anesthetized with a combination of sevoflurane (2%) and propofol (3 mg/kg/h). Anesthetized pigs were placed under C-arm, where 5F sheath (TerumoMedical) was introduced percutaneously to the femoral artery. Next, an angiographic catheter (5F, Balton) was navigated under X-ray guidance to the common carotid artery over hydrophilic 0.35 guidewire (Merit Laureate, Merit Medical). Microcatheter (UltraFlow™ HPC Flow Directed Micro Catheter, ev3™) was introduced over a micro guidewire (Hybrid 0,008", Balt) to the ascending pharyngeal artery with the tip placed proximally to the rete mirabile. Continuous flow flushing of heparinized (5000 U/l) saline was maintained to avoid occlusion of the microcatheter. Cells were transplanted under real-time MRI with the acquisition of dynamic T2*-weighted images (GE-EPI TR/TE:1750/30ms). The MRI protocol also included

T2 (TR/TE=5851/83ms) and T1 (TR/TE=1111.4/10 ms) scans prior and post cell delivery, SWI (TE/TR= 20/28) and diffusion-weighted with ADC mapping (TE/TR=104/4800) after transplantation to assess if the procedure and the cells caused brain damage.

MRI-guided intra-arterial transplantation of cGRPs and cMSCs

Eight dogs (5-12 years) of various breeds (1 German Shepherd, 3 Hovawart, 3 Bernese mountain, one crossbred dog) were divided into two groups: 1. with GRP transplantation (three animals) and 2. with cMSC transplantation (five animals). During the procedure, animals were anesthetized as described above. The 5-French introducer (ProCardia TerumoMedical) was inserted into the femoral artery and navigated to the carotid artery using fluoroscopy. Next, a 1.2-French microcatheter was advanced into the middle cerebral artery under roadmap guidance as described previously [32]. Then, dogs were transferred to a 3T MRI scanner (Magnetom Trio, Siemens) and positioned supine. MRI protocol was the same as that for pig studies with T2*-weighted dynamic imaging of cells biodistribution in real-time and T2, T1 scans prior and post cell delivery. Just after the procedure during recovery from anesthesia, dogs were hydrated with Ringer's fluid and were returned to their owners for recovery. The follow up monthly visits included blood analysis and neurological examination. MRI was done six months post-transplantation. For calculations of a brain covered by cells, Horos software was used.

Tissue samples

Brain tissues of pigs were collected immediately after slaughter, 24hours after pMSC transplantation, fixed in 4% paraformaldehyde, for 48 h at 4ºC, cryo-protected in 30% sucrose until sunk, frozen on dry ice for 5 min and kept at -80ºC for histological analysis. Brains from dogs that succumbed to the disease were harvested immediately after euthanasia (2 and 7 months post-transplantation), and each hemisphere was divided into two parts from which one was protected in liquid nitrogen and stored at -80 ºC for gene expression analysis and the other was protected for histology as described above. The rest of the transplanted dogs are still alive.

Histopathological analysis

For the detection of SPION labeled cells, Prussian Blue staining was performed. Porcine brain tissues were dried in RT for 10 min and washed in distilled water. The next sections were flooded in a mixture of equal parts of aqueous potassium ferrocyanide (5%) and aqueous hydrochloric acid (5%) for 30 min. Then sections were washed in distilled water three times for 5 min and counterstained with an aqueous solution of eosin for 1 min. After rinsing in distilled water, sections were dehydrated, cleared, and mounted in DPX (Sigma Aldrich). Sections were analyzed on a scanner (3D Histech).

Total RNA extraction and reverse transcription

Canine brain tissues form dogs that succumbed to disease were used for total RNA extraction using a commercial kit (A&A Biotechnology, Poland). The quality of RNA and its concentration was measured

using a NanoDrop 1000 spectrophotometer (Thermo Fisher Scientific Inc., DE, USA). Subsequently, reverse transcription reactions were done using the Reverse Transcription System Kit (Applied Biosystems, CA, USA). Two types of RT controls were used, one without RNA and another in the absence of the reverse transcriptase.

Real-time polymerase chain reaction (RT-PCR)

The cDNA obtained was used for real-time quantitative PCR analysis using the Applied Biosystems 7900HT Fast Real-Time PCR System (Applied Biosystems, USA). Each sample contained 3 µL (36 ng) cDNA, 1.5 µL RNAse-free water (Promega, USA), 5 µL TaqMan Universal MasterMix II (Life Technologies, USA) and 0.5 µL TaqMan assays (*MBP* -Cf02641118_m1, *GFAP*-Cf02655693_g1, *IBA*-Cf02653363_m1, *Olig1*-Cf02685151_s1, *MCT4*-Cf02702665_g1, *ChaT*-Cf02724445_m1, *RbFox3*-Cf02658562_m1, *GAPDH*-Cf04419463_gH, *β-actin-Cf04931159_m1*, *cyclophilin* (Cf02665149_m1. *Olig2* and *MCT2* were made to order; Life Technologies, USA). All PCR runs were performed as described previously.[4] Data obtained from the RT-PCR were normalized using the ratio of mRNA examined to the *GAPDH* mRNA. Quantification of gene expression was performed using the comparative CT method.

Statistical analysis

Statistical analyses were performed using GraphPad Prism 8.0 (GraphPad Software, Inc, San Diego, CA). The distribution of normality was evaluated with Kolmogorov-Smirnov test. The student's t-test was used to determine the difference in mRNA expression. The two-way ANOVA followed by Bonferroni's *post hoc* test was used to determine the size of hemispheres and ventricles and to assess differences between brain areas covered by MSC and GRP. All numerical data are presented as mean with standard deviation (SD) and differences were considered as statistically significant at the 95% confidence level ($P < 0.05$).

Declarations

Acknowledgements

We thank Krzysztof Mordwa and Adam Burczyk for help with animal procedures. This work was supported by the The National Centre for Research and Development (Strategmed 1/233209/12/NCBIR/2015).

Author contributions

Experimental design (IMC, DG, PW, MJ). Performing experiments (IMC, DG, LK, JK, MZ, JG, PH, KM). Preparation of cells (IMC, JS). Data collection (IMC, DG, LK, JK). Interpretation and processing of data (IMC, DG, LK, JK, PW, MJ). Writing manuscript (IMC, DG, LK, JK, MZ, JG, PH, JS, KM, ZA, PW, MJ). All authors read and approved the final manuscript.

Data availability

The datasets used and/or analyzed during the current study are available from the corresponding author on reasonable request.

Competing interests

PW, and MJ are founders of and hold equity in IntraArt. IM-C, DG, MZ, MJ and PW are founders and hold equity in Ti-Com. JS is founder of and hold equity in Sanford Biotech. All other authors declare that they have no conflict of interest.

References

1. Uccelli, A., Laroni, A. & Freedman, M.S. Mesenchymal stem cells as treatment for MS - progress to date. *Multiple sclerosis***19**, 515-519 (2013).
2. Silani, V., Cova, L., Corbo, M., Ciammola, A. & Polli, E. Stem-cell therapy for amyotrophic lateral sclerosis. *Lancet***364**, 200-202 (2004).
3. Golubczyk, D.*, et al.* The Role of Glia in Canine Degenerative Myelopathy: Relevance to Human Amyotrophic Lateral Sclerosis. *Mol Neurobiol***56**, 5740-5748 (2019).
4. Malysz-Cymborska, I.*, et al.* MRI-guided intrathecal transplantation of hydrogel-embedded glial progenitors in large animals. *Sci Rep***8**, 16490 (2018).
5. Kurtz, A. Mesenchymal stem cell delivery routes and fate. *International journal of stem cells***1**, 1-7 (2008).
6. Labusca, L., Herea, D.D. & Mashayekhi, K. Stem cells as delivery vehicles for regenerative medicine-challenges and perspectives. *World journal of stem cells***10**, 43-56 (2018).
7. Fischer, U.M.*, et al.* Pulmonary passage is a major obstacle for intravenous stem cell delivery: the pulmonary first-pass effect. *Stem cells and development***18**, 683-692 (2009).
8. Walczak, P.*, et al.* Dual-modality monitoring of targeted intraarterial delivery of mesenchymal stem cells after transient ischemia. *Stroke***39**, 1569-1574 (2008).
9. Janowski, M., Walczak, P. & Pearl, M.S. Predicting and optimizing the territory of blood-brain barrier opening by superselective intra-arterial cerebral infusion under dynamic susceptibility contrast MRI guidance. *Journal of cerebral blood flow and metabolism : official journal of the International Society of Cerebral Blood Flow and Metabolism***36**, 569-575 (2016).
10. Walczak, P.*, et al.* Real-time MRI for precise and predictable intra-arterial stem cell delivery to the central nervous system. *Journal of cerebral blood flow and metabolism : official journal of the International Society of Cerebral Blood Flow and Metabolism***37**, 2346-2358 (2017).
11. McGoldrick, P., Joyce, P.I., Fisher, E.M. & Greensmith, L. Rodent models of amyotrophic lateral sclerosis. *Biochimica et biophysica acta***1832**, 1421-1436 (2013).
12. Lyczek, A.*, et al.* Transplanted human glial-restricted progenitors can rescue the survival of dysmyelinated mice independent of the production of mature, compact myelin. *Experimental neurology***291**, 74-86 (2017).

13. Lepore, A.C.*, et al.* Human glial-restricted progenitor transplantation into cervical spinal cord of the SOD1 mouse model of ALS. *PloS one***6**, e25968 (2011).
14. Zhou, Y.Y., Yamamoto, Y., Xiao, Z.D. & Ochiya, T. The Immunomodulatory Functions of Mesenchymal Stromal/Stem Cells Mediated via Paracrine Activity. *Journal of clinical medicine***8**(2019).
15. Misra, V., Ritchie, M.M., Stone, L.L., Low, W.C. & Janardhan, V. Stem cell therapy in ischemic stroke: role of IV and intra-arterial therapy. *Neurology***79**, S207-212 (2012).
16. Saraf, J.*, et al.* Intra-arterial stem cell therapy modulates neuronal calcineurin and confers neuroprotection after ischemic stroke. *The International journal of neuroscience***129**, 1039-1044 (2019).
17. Walczak, P.*, et al.* Dual-modality monitoring of targeted intraarterial delivery of mesenchymal stem cells after transient ischemia. *Stroke***39**, 1569-1574 (2008).
18. Camstra, K.M.*, et al.* Canine Model for Selective and Superselective Cerebral Intra-Arterial Therapy Testing. *Neurointervention* (2020).
19. Lundberg, J.*, et al.* Targeted intra-arterial transplantation of stem cells to the injured CNS is more effective than intravenous administration: engraftment is dependent on cell type and adhesion molecule expression. *Cell transplantation***21**, 333-343 (2012).
20. Chua, J.Y.*, et al.* Intra-arterial injection of neural stem cells using a microneedle technique does not cause microembolic strokes. *J Cereb Blood Flow Metab***31**, 1263-1271 (2011).
21. Gorelik, M.*, et al.* Use of MR cell tracking to evaluate targeting of glial precursor cells to inflammatory tissue by exploiting the very late antigen-4 docking receptor. *Radiology***265**, 175-185 (2012).
22. Jablonska, A.*, et al.* Overexpression of VLA-4 in glial-restricted precursors enhances their endothelial docking and induces diapedesis in a mouse stroke model. *J Cereb Blood Flow Metab***38**, 835-846 (2018).
23. Nitzsche, F.*, et al.* Concise Review: MSC Adhesion Cascade-Insights into Homing and Transendothelial Migration. *Stem cells***35**, 1446-1460 (2017).
24. Guzman, R., Janowski, M. & Walczak, P. Intra-Arterial Delivery of Cell Therapies for Stroke. *Stroke***49**, 1075-+ (2018).
25. Janowski, M.*, et al.* Cell size and velocity of injection are major determinants of the safety of intracarotid stem cell transplantation. *J Cerebr Blood F Met***33**, 921-927 (2013).
26. Cui, L.L.*, et al.* The cerebral embolism evoked by intra-arterial delivery of allogeneic bone marrow mesenchymal stem cells in rats is related to cell dose and infusion velocity. *Stem cell research & therapy***6**(2015).
27. Lu, S.S.*, et al.* In Vivo MR Imaging of Intraarterially Delivered Magnetically Labeled Mesenchymal Stem Cells in a Canine Stroke Model. *PloS one***8**(2013).
28. Youn, S.W.*, et al.* Feasibility and Safety of Intra-arterial Pericyte Progenitor Cell Delivery Following Mannitol-Induced Transient Blood Brain Barrier Opening in a Canine Model. *Cell transplantation***24**, 1469-1479 (2015).

29. Karp, J.M. & Leng Teo, G.S. Mesenchymal stem cell homing: the devil is in the details. *Cell stem cell***4**, 206-216 (2009).
30. Lo Sicco, C.*, et al.* Mesenchymal Stem Cell-Derived Extracellular Vesicles as Mediators of Anti-Inflammatory Effects: Endorsement of Macrophage Polarization. *Stem cells translational medicine***6**, 1018-1028 (2017).
31. Lovett, M.C.*, et al.* Quantitative assessment of hsp70, IL-1beta and TNF-alpha in the spinal cord of dogs with E40K SOD1-associated degenerative myelopathy. *Veterinary journal***200**, 312-317 (2014).
32. Golubczyk, D.*, et al.* Endovascular model of ischemic stroke in swine guided by real-time MRI. *Scientific reports***10**, 17318 (2020).

Figures

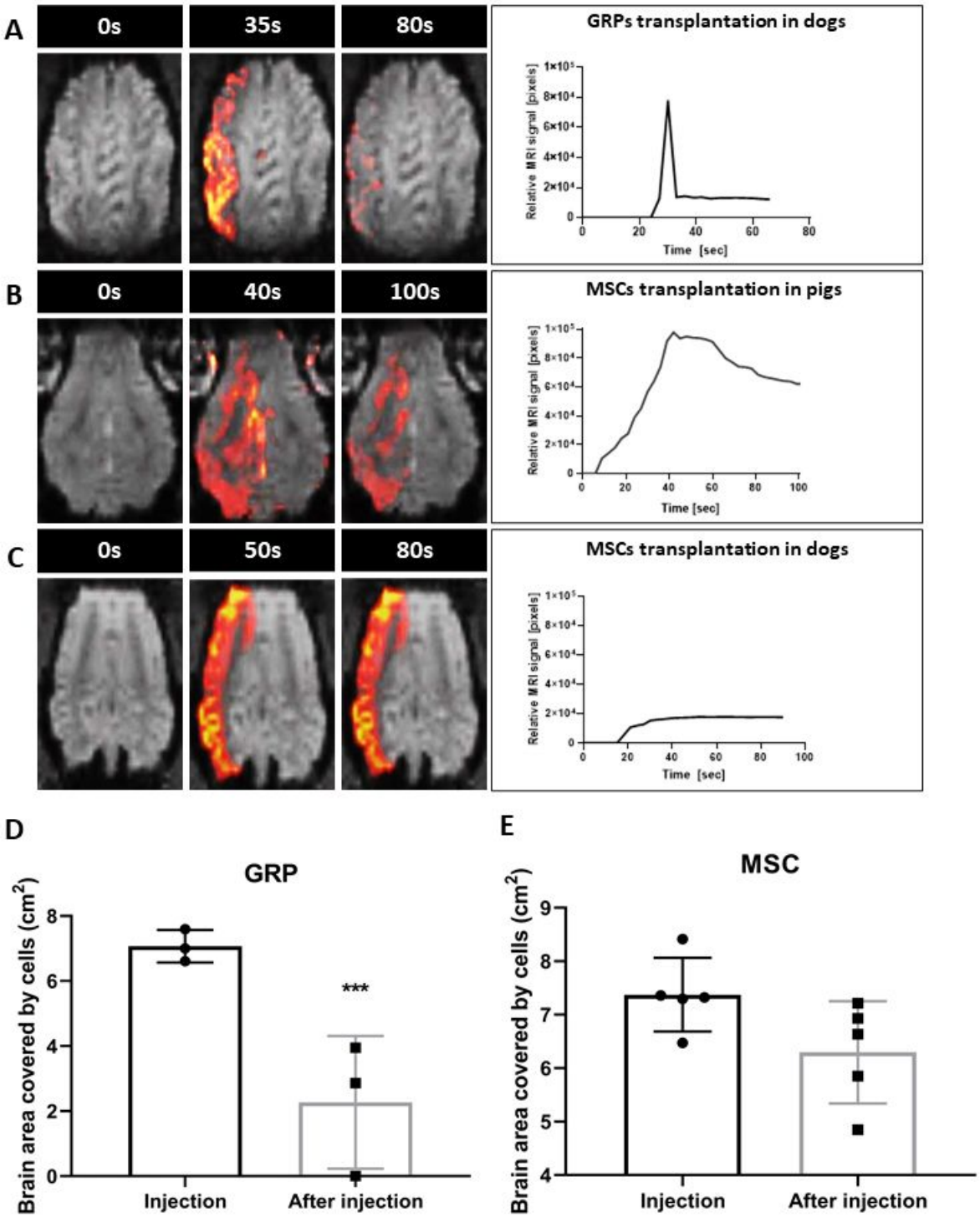

Figure 1

MRI – guided transplantation of stem cells. (A) MRI-guided intraarterial transplantation of SPION labeled canine GRPs in DM dogs. (B) MRI-guided intraarterial transplantation of SPION labeled porcine MSCs in pig. (C) MRI-guided intraarterial transplantation of SPION canine MSCs in DM dogs. (D) Brain area covered by transplanted GRP cells during and post injection in DM dogs. (E) Brain area covered by transplanted MSC cells during and post injection in DM dogs.

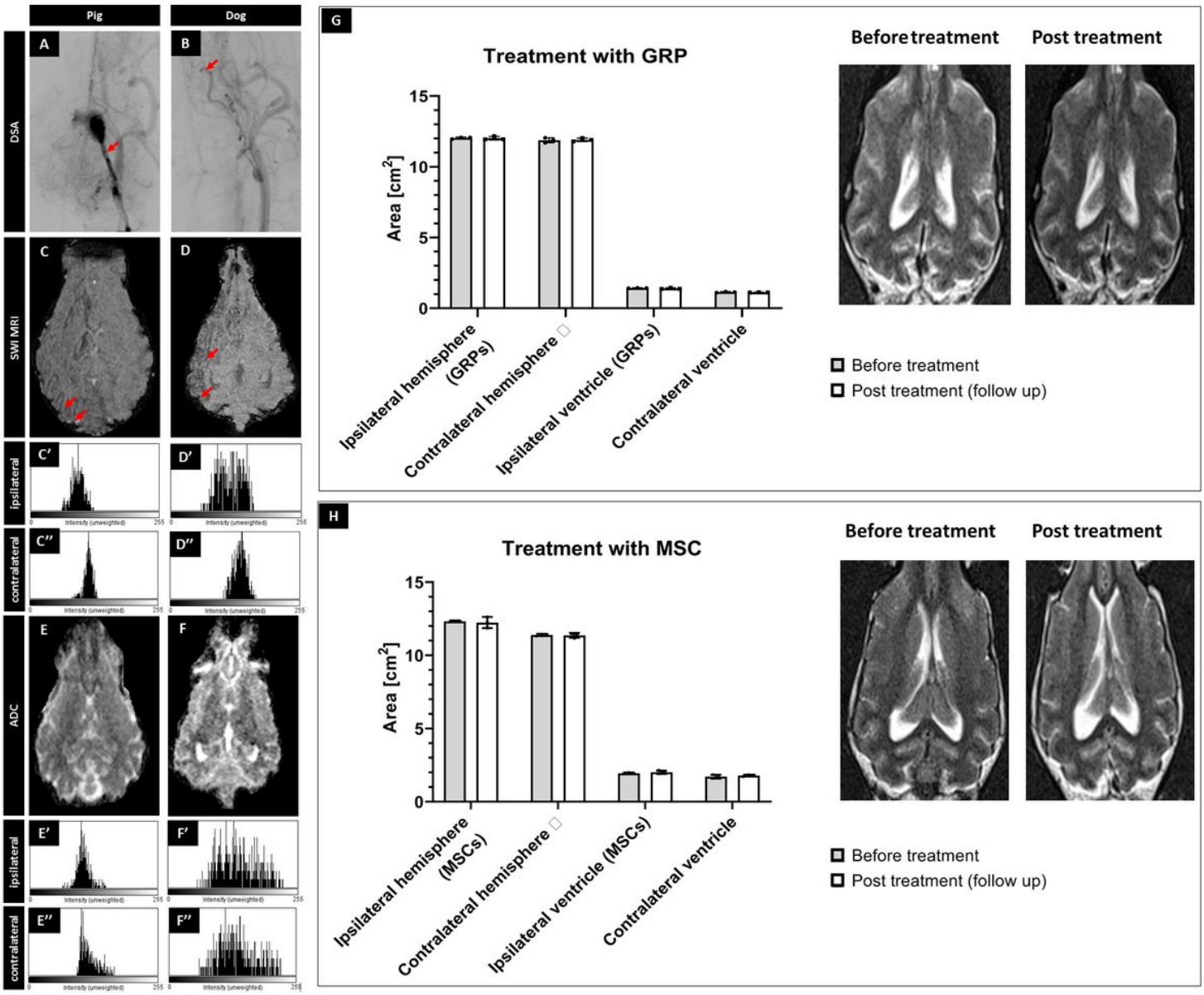

Figure 2

Safety of the procedures. X-ray evaluation of catheter placement (A & B; arrows indicate placement of the tip of microcatheter). SWI (C & D) with histograms from ipsilateral (C' and D') and contralateral (C" and D") hemisphere. ADC scans (E and F) after pig's and canine's MSC transplantation with histograms from ipsilateral (E' and F') and contralateral (E" and F") hemisphere. Evaluation of size of hemispheres and ventricles visible on the MRI before versus post-transplantation of GRPs (G) and MSCs (H).

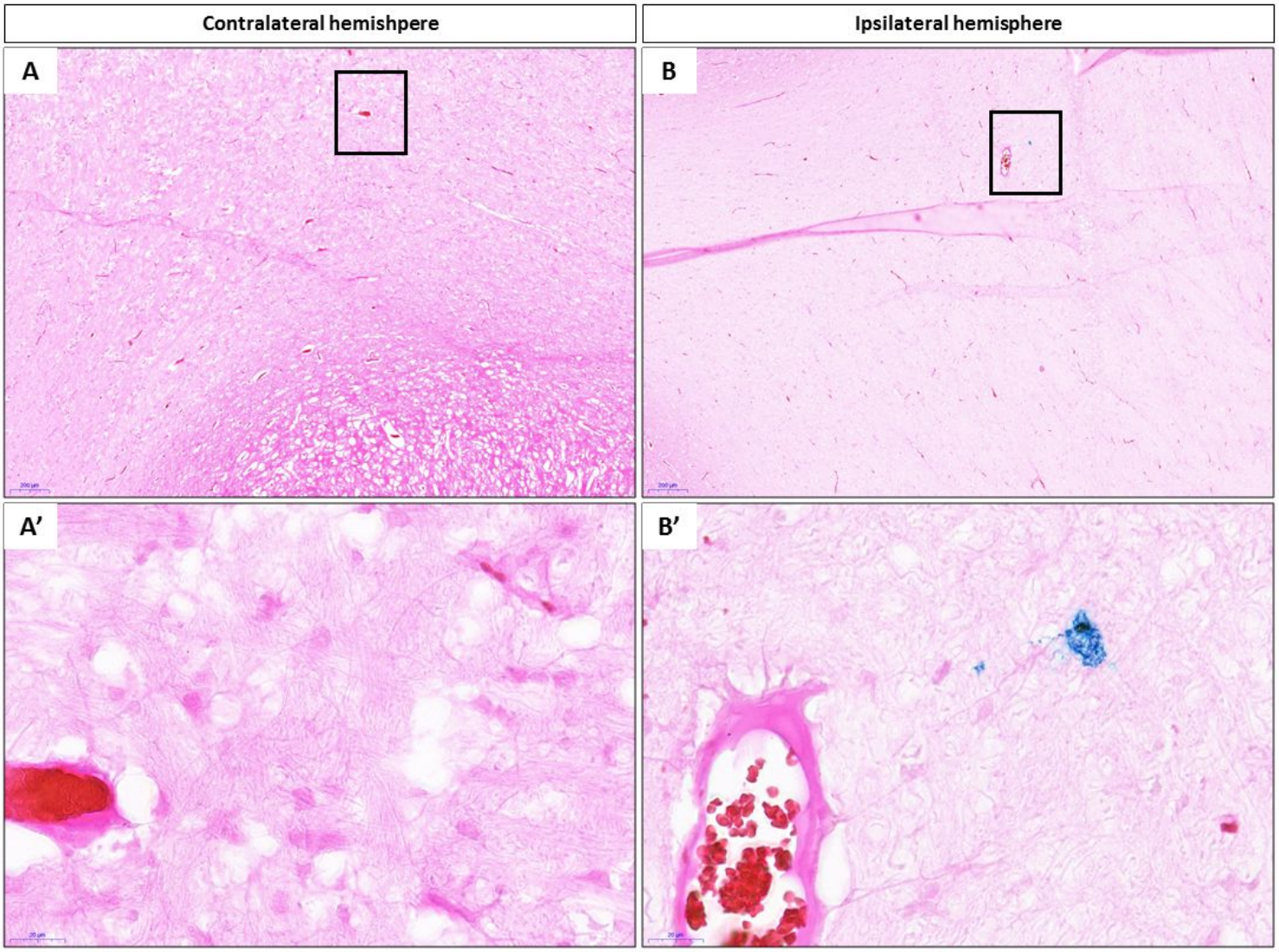

Figure 3

Histological evaluation. Prussian blue staining of brain of pigs after SPION pMSCs transplantation in contralateral (A – x5 magnification, A' – x40 magnification) and ipsilateral hemisphere (B – x5, B'– x40 magnification).

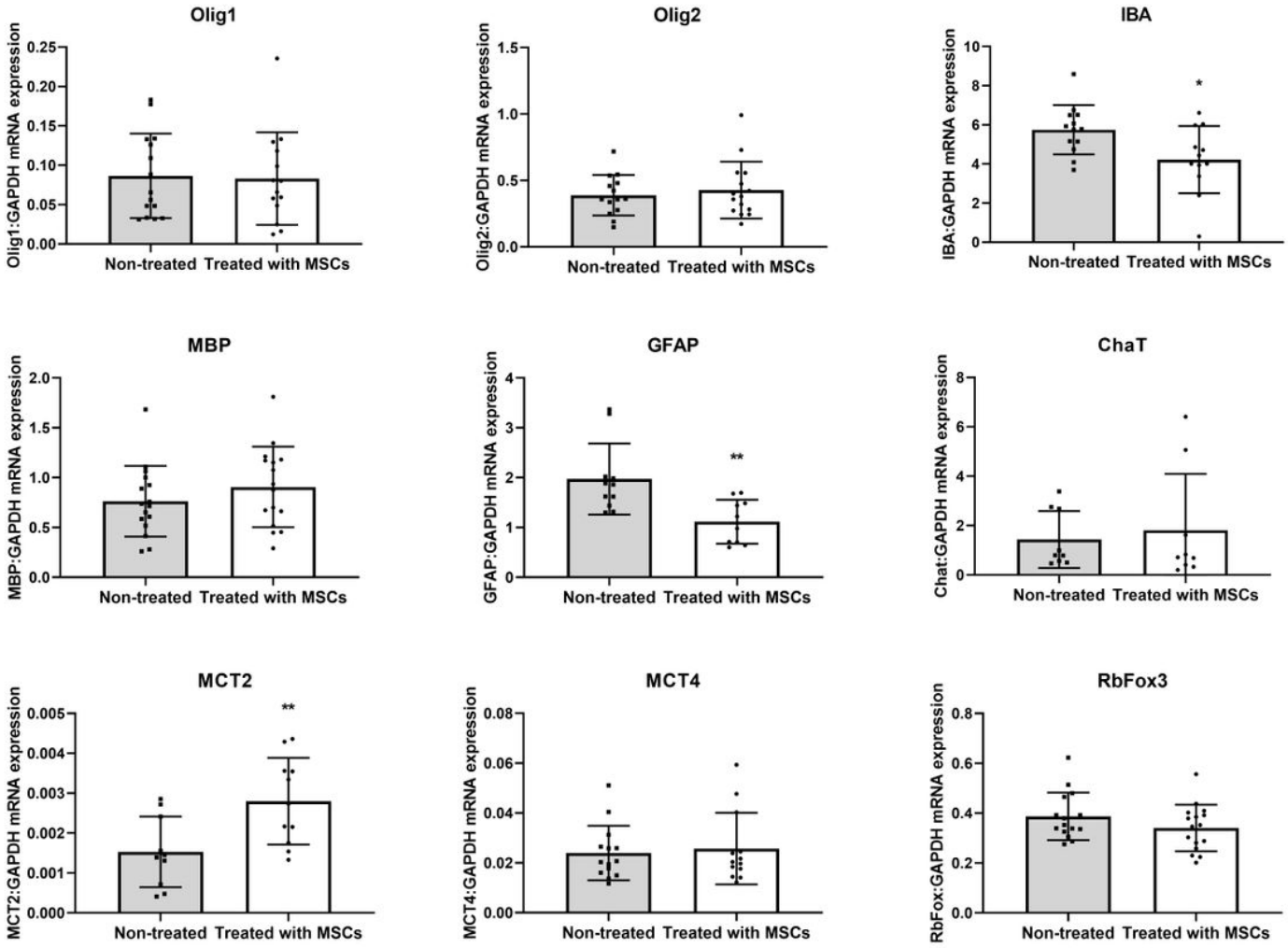

Figure 4

Real – time PCR analysis. Effect of canine MSCs transplantation on Olig1, Olig2, IBA, MBP, GFAP, Chat, MCT2, MCT4 and RBFox3 mRNA expression in the brains of DM dogs.

Supplementary Files

This is a list of supplementary files associated with this preprint. Click to download.

- Supplementaryfile.pdf